P4.10 AVHRR/MODIS RELATIVE CALIBRATION BIAS ESTIMATES DEDUCED FROM THE SNO METHOD: UNCERTAINTIES DUE TO EARTH-SCENE INHOMOGENEITIES

*Robert A. Iacovazzi, Jr.[1], Changyong Cao[2], and Pubu Ciren[3]
[1]Earth Resources Technology, Inc., Jessup, MD
[2]NOAA/NESDIS/ORA, Camp Springs, MD
[3]QSS Group, Lanham, MD

ABSTRACT

The Simultaneous Nadir Overpass (SNO) method estimates the magnitude of relative calibration biases between two similar radiometers flown on different polar-orbiting satellites. For this purpose, the SNO method uses radiometer measurements taken from satellite overpasses of a given earth location that occur within 30 seconds of each other. This reduces uncertainties of intersatellite radiometer calibration bias estimates that can result from change of the atmosphere, land, and/or ocean within the time period between satellite overpasses. On the other hand, several uncertainties remain in the SNO method that are mainly related to a combination of instrument differences and earth-scene spatial/temporal inhomogeneities. Since these uncertainties need to be understood and quantified in order to increase confidence in the SNO method, we explore in this study earth-scene inhomogeneity related uncertainties of intersatellite calibration biases estimated from 22 August to 22 October 2005 SNOs occurring between Polar-orbiting Operational Environmental Satellite (POES) Advanced Very High Resolution Radiometer (AVHRR) and the Earth Observing System (EOS) Moderate Resolution Imaging Spectroradiometer (MODIS).

1. INTRODUCTION

Ideally, identical radiometers flown on different satellites that simultaneously view the same exact earth target should produce redundant observations. Any deviation from these results would be attributable to relative calibration differences between the "identical" radiometers. Taking advantage of this concept, the Simultaneous Nadir Overpass (SNO) method was developed to estimate and track relative calibration biases between radiometers flown onboard different polar-orbiting satellites (*e.g.*, Cao *et al.*, 2002, 2004, and 2005). For a given pair of polar-orbiting satellites, the essence of the SNO method is to minimize earth-scene-related differences found between instrument measurements. This is done by utilizing near-nadir data close to satellite orbital intersections (OIs) that have a relatively small time difference. For this study, an OI is considered to be an SNO when the time difference of the nadir overpass of two satellites at the OI is less than 30 seconds. Also, we use only those observations that fall within about 200 km of the SNO location.

Although SNO observations improve substantially estimates of relative calibration biases, the fact that the SNO method relies on *near-simultaneous* observations from *similar* radiometers leads to uncertainties in the method. For example, *similar* radiometers can introduce uncertainties through instrument modulation transfer function (MTF), spectral response function (SRF), and geolocation discrepancies. In addition, since the instruments are not flown on the same satellite, uncertainties resulting from instrument view-angle and pixel location mismatches can be present. Furthermore, *near-simultaneous* observations introduce uncertainties related to time of measurement discrepancies. The plethora of mechanisms mentioned here offer several pathways to generate uncertainties in intersatellite calibration bias estimates. On the other hand, the degree to which they are manifested in the data is often related to a single factor: earth-scene variability in space and time. These uncertainties in the SNO method that are dependent upon earth-scene spatial/temporal inhomogeneities need to be carefully studied and eventually accounted for.

This year, we initiated the development of automated software that can create and analyze SNO datasets from POES and EOS in near real time. This new software is currently designed to process AVHRR and MODIS data from SNO events between POES NOAA18 (N18) and EOS Aqua (AQUA) satellites, respectively, and can be readily expanded to accommodate SNO events from any satellite instrument pair. AQUA MODIS and N18 AVHRR were chosen for initial software development because of their importance to National Polar-orbiting Operational Environmental Satellite System (NPOESS) risk reduction activities. In this extended abstract, we utilize the SNO data from these satellite instruments to explore the uncertainties of relative calibration bias estimates that are related to earth-scene spatial/temporal inhomogeneities. In the next section, characteristics of SNO data from N18/AVHRR and AQUA/MODIS are presented. In Section Three (Four) the relationship of earth-scene spatial (temporal) inhomogeneities on the difference between the N18/AVHRR and AQUA/MODIS data are shown. In Section Five, a discussion of the results is given.

[*] *Corresponding author address:* Robert A. Iacovazzi, Jr., NOAA/NESDIS/ORA, Room 7215, NOAA Science Center, 5200 Auth Road, Camp Springs, MD 20746. E-mail: Bob.Iacovazzi@noaa.gov

2. N18/AVHRR and AQUA/MODIS SNO DATA

SNO events between N18/AVHRR and AQUA/MODIS during the period from 22 August to 22 October 2005 are given in Table 1. As mentioned earlier, these SNO events have been chosen based on the criteria that the nadir observations of the two instruments are taken less than 30 seconds apart, and lie within approximately 200 km, from the SNO location. An example of a typical SNO is revealed in Figure 1 using the AVHRR Global Area Coverage (GAC) and MODIS 12 μm images taken from the 24 August 2005 SNO. Note that AVHRR GAC data are used in this study, and the MODIS 1 km data have been interpolated to the AVHRR GAC pixels, which crudely have a 4 km resolution. As expected from nearly-simultaneous observations, the two images in Figure 1 show excellent qualitative agreement.

Table 1: SNO Events between NOAA18/AVHRR and AQUA/MODIS for the period 22 August to 22 October 2005. Note that longitude is relative to 0^0 E (Greenwich Meridian), and latitude is relative to 0^0 N (Equator).

Month	*Day*	*Hour*	*Min*	*Latitude*	*Longitude*
8	22	16	6	80.0	267.3
8	24	20	0	-79.8	29.8
9	2	12	30	80.0	320.0
9	4	16	25	-79.6	85.0
9	6	20	20	80.2	201.9
9	9	0	14	-80.2	322.4
9	11	4	9	79.6	89.4
9	13	8	4	-80.1	206.5
9	15	11	58	79.8	330.0
9	26	8	23	79.8	23.6
9	28	12	17	-79.5	148.2
10	2	20	7	-79.9	26.7
10	5	0	2	80.1	146.1
10	7	3	56	-79.9	269.3
10	9	7	51	80.1	28.9
10	15	20	26	80.2	199.6
10	18	0	20	-79.4	327.6
10	20	4	15	79.5	88.2

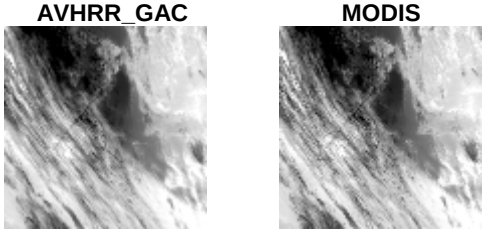

Figure 1: AVHRR_GAC and MODIS 12 μm images taken from the 24 August 2005 SNO.

In Figures 2P1-2P5, scatterplots are presented of albedo (brightness temperature (Tb)) differences between MODIS and AVHRR as a function of AVHRR albedo (Tb). These five scatterplots respectively represent results from the AVHRR/MODIS spectral band pairs centered at 0.63/0.645 (P1), 0.912/0.858 (P2), 3.74/3.75 (P3), 10.80/11.0 (P4), and 12.0/12.0 (P5) μm. Note that the 1.61/1.64 μm channel pair could not be examined due to lack of valid 1.64 μm measurements in the AQUA MODIS datasets for this time period. Each scatterplot point symbolizes the mean value of all pixels for a given SNO listed in Table 1. Although a limited number of data are presented, the most striking result of these figures is that albedo (Tb) differences can be a function of albedo (Tb).

In the P1 (P2) reflective band pair, the slope of the linear regression between MODIS/AVHRR albedo difference and AVHRR albedo in the Northern Hemisphere (NH) is 0.15 (0.20), and this slope is statistically different from zero slope at the 99 % confidence level (see von Storch and Zwiers (1999) for discussion of confidence determination). Since the intercepts (not given) are near or above zero, this means that MODIS NH albedos in P1 (P2) are roughly 15 % (20 %) higher than those in AVHRR. There are not any Southern Hemisphere (SH) results for these spectral band pairs, because SNOs typically occur between 70^o and 80^o of latitude, and sunlit earth scenes are rare in the SH during the time frame of these observations. The correlation between NH MODIS/AVHRR albedo difference and AVHRR albedo in Figures 2P1 and 2P2 are 0.85 and 0.84, respectively. These correlations are different from zero at the 99 % confidence level, and both translate to an average explained variance – *i.e.*, square of the correlation – of about 70 %. Therefore, the amount of unexplained variance is about 30 %, which may be due to earth-scene spatial/temporal inhomogeneities.

In the mainly emissive P3-P5 band pairs, the MODIS/AVHRR Tb difference usually increases as AVHRR Tb decreases. Also, in the SH the rate of increase can be different than that in the NH. This can be quantified using the slope of the regression between the MODIS/AVHRR Tb difference and AVHRR Tb. For band pairs P3/P4/P5, these slopes are respectively 0.02/-0.02/-0.01 for the NH and -0.11/-0.04/-0.03 for the SH. Meanwhile, the correlations associated with the regression are 0.50/-0.76/-0.66 for the NH and -0.91/-0.94/-0.99 for the SH. All of the slopes and correlations for the SH are statistically different than zero at the 99 % confidence level, while those for the NH are not. The insignificant correlations in the NH may be a result of a relatively small range of MODIS/AVHRR Tb difference coupled with errors associated with relatively large earth-scene spatial variability, which is due to an often complex mix of land, ocean, and ice at the surface between 70^o N and 80^o N latitude. In addition, the relatively large slope in the SH data of Figure 2P3 during this observation time frame may be a result of very low sensitivity of the P3 bands to terrestrial radiation when Tbs are very cold (~ 210 K).

These results indicate calibration differences between N18/AVHRR and AQUA/MODIS could be the cause of the albedo or Tb dependence of the difference values shown in the figures. On the other hand, it is also important to explore possible discrepancies

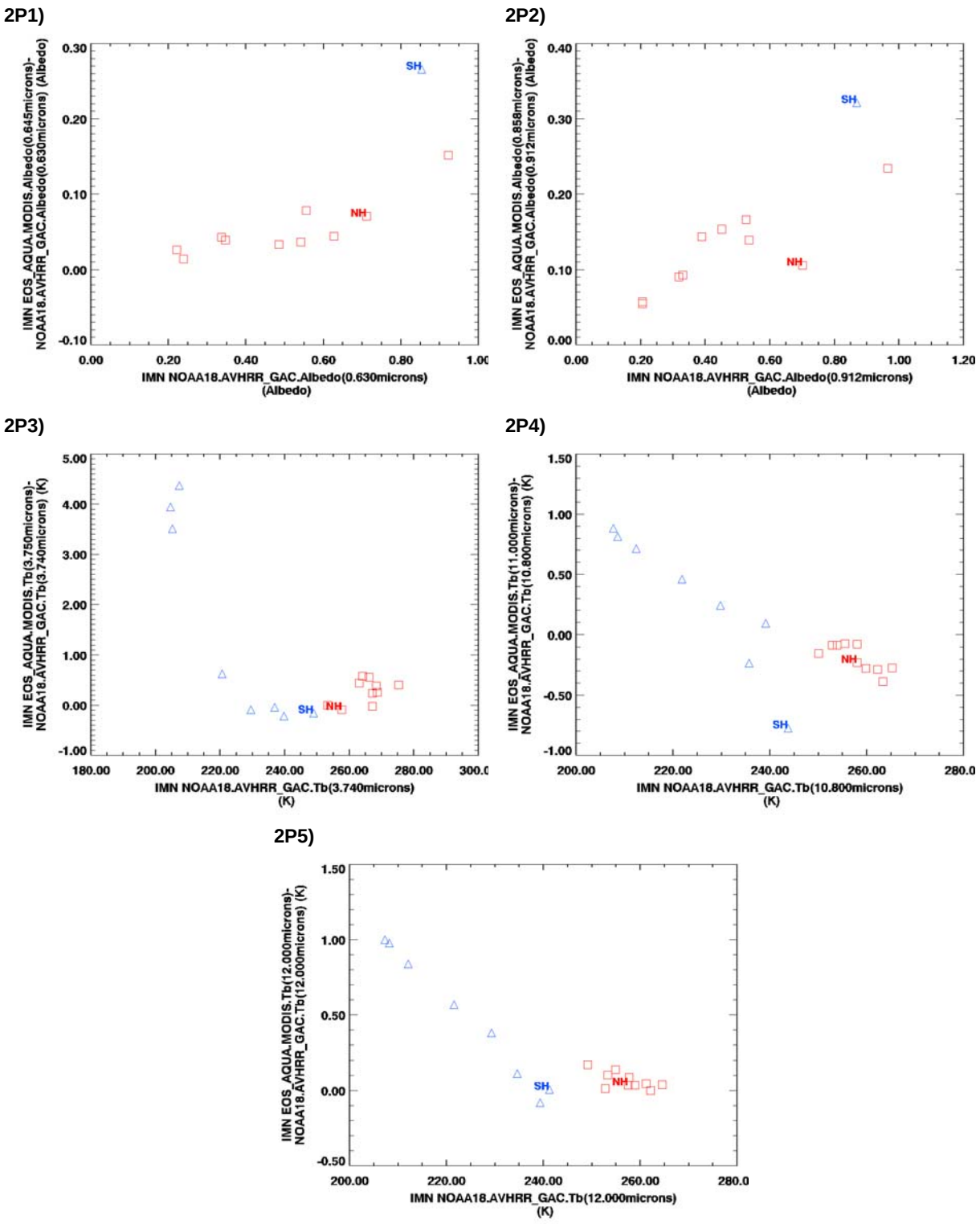

Figure 2: Scatterplots of MODIS/AVHRR albedo (brightness temperature (Tb)) differences as a function of AVHRR albedo (Tb). These five scatterplots respectively represent results from the AVHRR/MODIS spectral band pairs centered at **P1)** 0.63/0.645, **P2)** 0.912/0.858, **P3)** 3.74/3.75, **P4)** 10.80/11.0, and **P5)** 12.0/12.0 μm. Each scatterplot point symbolizes the mean value of all pixels for a given SNO listed in Table 1.

between the datasets associated with spatial/temporal inhomogeneities of the earth scene views.

3. EARTH-SCENE SPATIAL INHOMOGENEITIES

Earth-scene spatial inhomogeneities create differences between satellite instrument measurements at an SNO because the instruments are observing radiation from different physical locations. Observations of radiation from the surface or a given layer of the atmosphere can differ between satellite instruments if the pixel locations are not coincident, the MTFs are not identical, or there are errors in geolocation. Altitude displacement of the region of observed radiation can occur if view-angles, spectral bands and/or SRFs are not the same. Therefore, uncertainties arising from earth-scene spatial inhomogeneities are a function of our ability to interpolate the SNO measurements of one satellite instrument into the observation reference frame of the other.

Spatial interpolation of a data set has no errors if there are no spatial variations of the quantity being interpolated. On the other hand, as complex gradients of the quantity arise, so do errors in interpolation. Thus, the variability of the difference measurements from two SNO instruments may depend roughly upon the degree of variability of the earth scene. To show this, in Table 2 we give the correlation values associated with the regression between the standard deviation (SD) of the MODIS/AVHRR albedo (Tb) differences as a function of the SD of AVHRR albedo (Tb). In this table, the 0.95 (0.94) correlation associated with reflective band pair P1 (P2) is different from zero at the 99 % confidence level, and explains 88 % (90 %) of the variance of the SD of MODIS/AVHRR albedo difference. Why these results degrade substantially for the emissive channels is a question left for future research.

Table 2: Correlation values of the linear regression between the SD of the MODIS/AVHRR albedo (Tb) differences and the SD of AVHRR albedo (Tb).

Region	***P1***	***P2***	***P3***	***P4***	***P5***
NH	0.95	0.94	0.76	-0.03	0.06
SH	N/A	N/A	0.23	0.37	0.40

In Figures 3P1-3P5, scatterplots of albedo (Tb) differences between MODIS and AVHRR as a function of the SD of AVHRR albedo (Tb) are shown in order to expose possible relationships between the magnitude of the albedo (Tb) differences and spatial variability. From these figures, it is found that albedo (Tb) difference is not a clear function of the SD of albedo (Tb) for band pairs P2-P5. In these cases, neither the slopes nor correlations (not given) associated with least squares linear regression are statistically different from zero at the 99 % confidence level. On the other hand, the NH P1 spectral band pair has a correlation and slope of 0.82 and 0.17, respectively, and both of these values are statistically significant at the 99 % confidence level. This indicates that spatial variability has the strongest link to the difference values in the NH P1 case.

In the SH data in Figure 3P3, it is noteworthy to observe the three points with relatively large Tb difference in the upper portion of the plot. According to Figure 2P3, these points also have extremely low AVHRR Tb, which may be near the instruments level of detection threshold for the bands. Therefore, a screening technique may be necessary on the SNO method to eliminate data in the near infrared portion of the spectrum when the scene is relatively cold and not illuminated by the sun.

From these results, significant impact of the spatial variability on the slope of the regression line between MODIS/AVHRR albedo differences and AVHRR albedo shown in Figure 2P1 cannot be ruled out. On the other hand, in the P2-P5 band pairs similar significant impacts from variability in the earth scene are not discernable from this analysis.

4. EARTH-SCENE TEMPORAL INHOMOGENEITIES

Temporal variability of the earth scene can bring about significant differences between satellite data measurements. For this reason, the SNO method attempts to minimize the time difference between satellite observations. On the other hand, the earth system does not even rest for 30 seconds, which is the time limit chosen to classify an OI as an SNO in this study. In this period of time, there can be changes in the earth system that impact the albedo or Tb difference value between data sets.

In order to crudely assess the impact that observation time difference has on satellite measurements, the correlation of the linear regression between the SD of MODIS/AVHRR albedo (Tb) difference and observation time difference is given in Table 3. From this table, it is found that the correlations values are relatively small. In addition, none of the correlations presented in Table 3 can be considered statistically different than zero at the 99 % level. On the other hand, since SD of albedo (Tb) difference does not necessarily characterize the albedo (Tb) bias, exploring the relationship between mean albedo (Tb) difference and measurement time difference is necessary.

Table 3: Correlation values of the linear regression between the SD of MODIS/AVHRR albedo (Tb) difference and observation time difference.

Region	***P1***	***P2***	***P3***	***P4***	***P5***
NH	0.03	-0.07	0.38	-0.11	-0.05
SH	N/A	N/A	0.25	-0.28	-0.28

In Figures 4P1-4P5, scatterplots of albedo (Tb) differences between MODIS and AVHRR as a function of observation time difference are shown for the SNO events listed in Table 1 in order to expose possible relationships between the magnitude of the albedo (Tb) differences and the time difference between satellite measurements. From these figures, it is found that albedo (Tb) difference usually does not have a coherent relationship with observation time difference. The

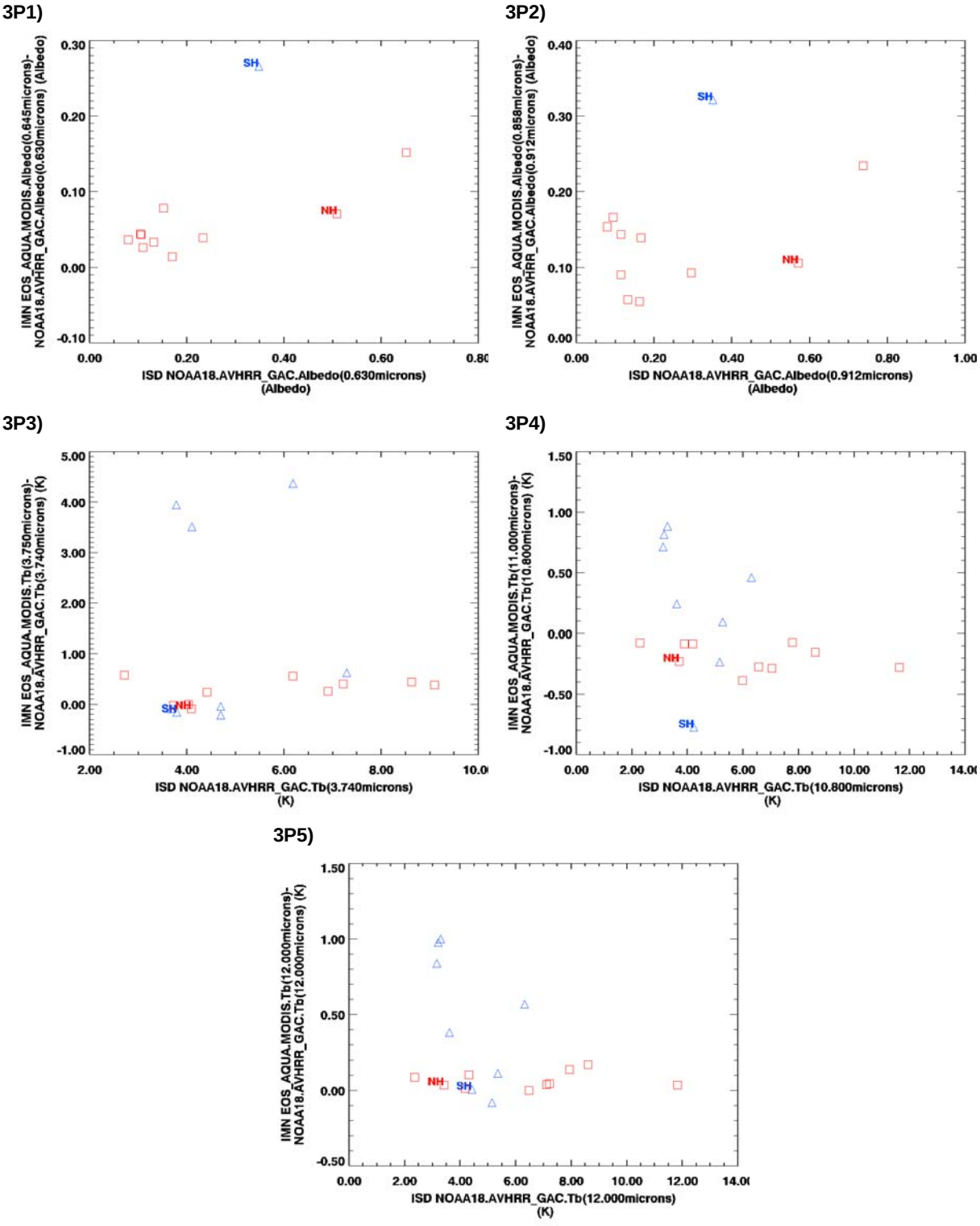

Figure 3: Scatterplots of MODIS/AVHRR albedo (Tb) differences as a function of the SD of AVHRR albedo (Tb). These five scatterplots respectively represent results from the AVHRR/MODIS spectral band pairs centered at **P1)** 0.63/0.645, **P2)** 0.912/0.858, **P3)** 3.74/3.75, **P4)** 10.80/11.0, and **P5)** 12.0/12.0 μm. Each scatterplot point symbolizes the statistical value of all pixels for a given SNO listed in Table 1.

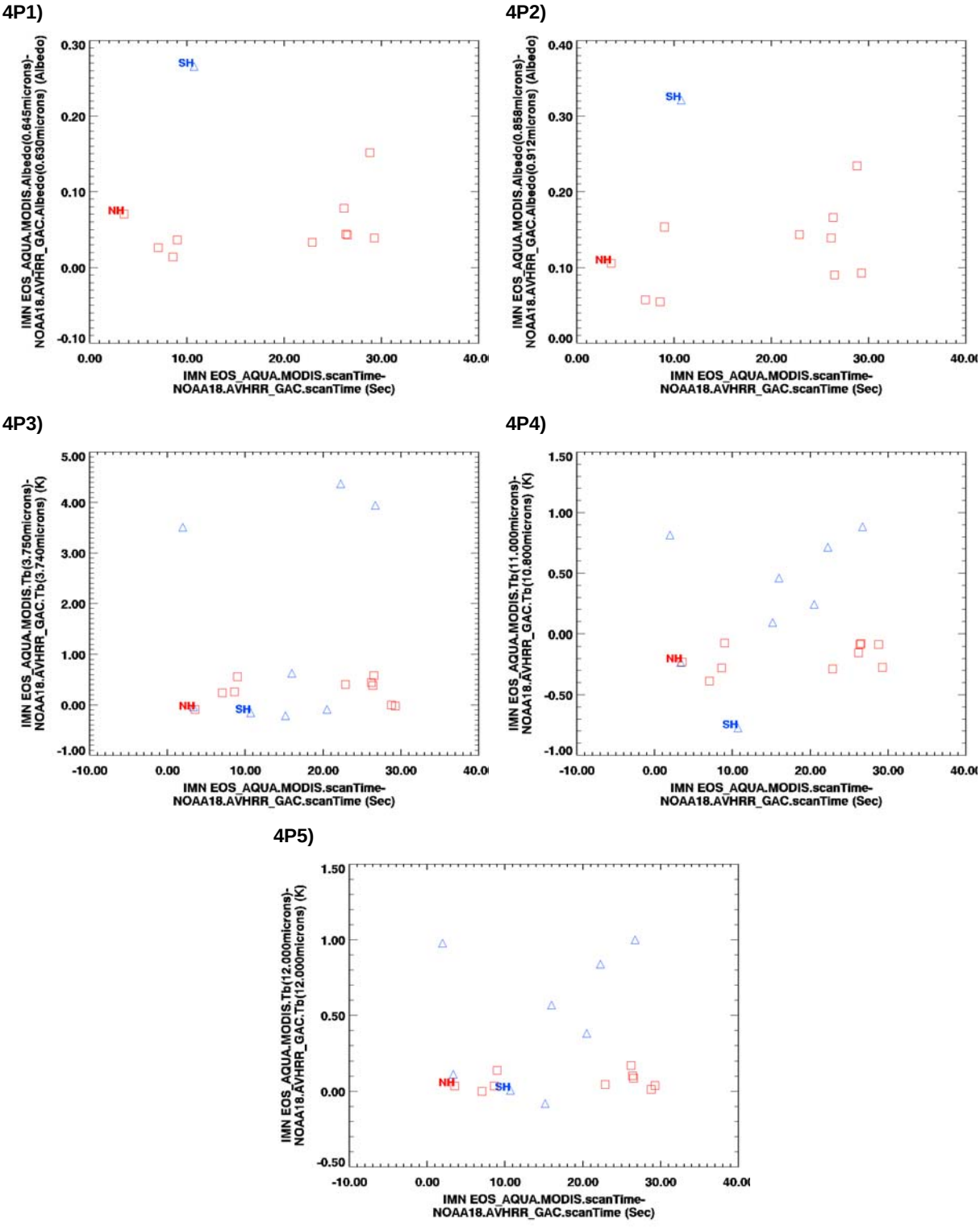

Figure 4: Scatterplots of MODIS/AVHRR albedo (Tb) differences as a function of observation time difference. These five scatterplots respectively represent results from the AVHRR/MODIS spectral band pairs centered at **P1)** 0.63/0.645, **P2)** 0.912/0.858, **P3)** 3.74/3.75, **P4)** 10.80/11.0, and **P5)** 12.0/12.0 μm. Each scatterplot point symbolizes the statistical value of all pixels for a given SNO listed in Table 1.

strongest correlation between MODIS/AVHRR albedo (Tb) difference and observation time difference is 0.49 in the NH P2 band pair, but this correlation is not significant at the 99 % confidence level. Thus, in this analysis, OI observation time differences of less than 30 seconds cannot be assumed to significantly impact the linear change of MODIS/AVHRR albedo (Tb) difference as a function of AVHRR albedo (Tb) found in Figures 2P1-2P5.

5. DISCUSSION

The impact of spatial/temporal earth-scene inhomogeneities on the difference between MODIS and AVHRR albedo (Tb) measurements at SNO locations has been briefly examined for AVHRR/MODIS band pairs centered at 0.63/0.645 (P1), 0.912/0.858 (P2), 3.74/3.75 (P3), 10.80/11.0 (P4), and 12.0/12.0 (P5) μm. It is found that such impacts may be a factor in explaining the increase of MODIS/AVHRR albedo difference as AVHRR albedo increases for the NH P1 band pair (see Figure 2P1), while they are not considered significant for other band pairs. This leads us to attempt to give plausible explanations for the significant slopes associated with linear regression between MODIS/AVHRR albedo difference and AVHRR albedo in the NH shown in Figures 2P1-2P2, and between MODIS/AVHRR Tb difference and AVHRR Tb in the SH shown in Figures 2P3-2P5.

In the solar reflective bands - P1 and P2 - the MODIS instrument is calibrated on-orbit with respect to the sun (Guenther *et al.*, 1996). On the other hand, the AVHRR instrument depends on a pre-launch calibration that is updated periodically on-orbit with the aid of vicarious calibration with respect to a scene in the Sahara Desert (Slater *et al*., 1987). If the assumed albedo from the desert target is unrealistically low then the gain for the AVHRR channel could be artificially small by a relatively consistent fraction compared to MODIS. In addition, since the SRFs of the AVHRR and MODIS are not the same in the P1 and P2 bands, and if the reflectance of the earth near the poles is consistently higher in those spectral regions not covered by AVHRR, then one would expect MODIS to have higher albedo values. Such hypotheses could be tested using radiative transfer models, and is a subject for future work.

In the SH during the time of observations used in this study, spectral band pairs P3-P5 primarily measure infrared emission from the earth's surface. A potential reason for the slopes found between MODIS/AVHRR Tb difference and AVHRR Tb are unresolved non-linearities in the instrument response that are not captured in the calibration equations of MODIS and/or AVHRR. In addition, it is possible that the character of the warm-blackbody is not fully understood. For example, the AVHRR blackbody is known to have contamination problems (Cao, *et al.,* 2001). In Figures 5P4 and 5P5, we show plots of the regression line slope of AVHRR Tb versus MODIS Tb as a function of Mean AVHRR Tb, where each point in the figure represents statistics based on data from a single SNO listed in Table 1. These plots show clearly that the slope between AVHRR and MODIS Tb gets smaller as the average temperature of a given SNO data set increases. This hints that an uncaptured non-linearity may exist in the MODIS and/or AVHRR calibration equations. This also is a subject of future work.

P4)

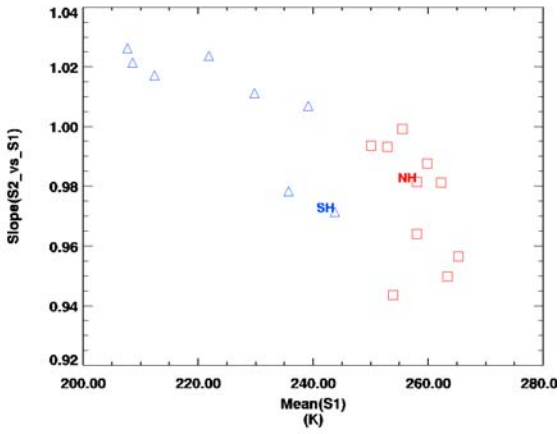

P5)

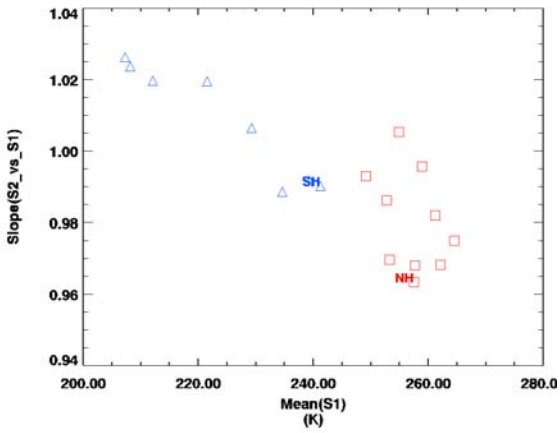

Figure 5: Scatterplots of the regression line slope of AVHRR Tb (S1) versus MODIS Tb (S2) as a function of Mean AVHRR Tb. Plots are given for **P4)** 10.80/11.0 and **P5)** 12.0/12.0 μm spectral band pairs, and each point in the figure represents statistics based on data from a single SNO listed in Table 1.

In this study, we focused mainly on spatial/temporal earth-scene variabilities that may cause MODIS/AVHRR albedo (Tb) difference to be a linear function of AVHRR albedo (Tb). On the other hand, there could be substantial random variability in the albedo (Tb) difference versus albedo (Tb) relationship associated with earth-scene inhomogeneities. These random variabilities are offered in Table 4 through the aid of the SD of error associated with linear regression of MODIS/AVHRR albedo (Tb) difference as a function of AVHRR albedo (Tb) in Figures 2P1-2P5. Although random variability has less impact on long-term intersatellite calibration, information about the

instruments and earth-scene inhomogeneity may also be gained from intense research of random variability in satellite data measurements at SNOs.

Table 4: SD of error associated with linear regression of albedo (Tb) difference as a function of albedo (Tb).

Region	***P1 (albedo)***	***P2 (albedo)***	***P3 (K)***	***P4 (K)***	***P5 (K)***
NH	0.02	0.03	0.21	0.07	0.04
SH	N/A	N/A	0.83	0.20	0.05

REFERENCES

Cao, C., H. Xu, J. Sullivan, L. McMillin, P. Ciren, and Y. Hou, 2005: Intersatellite radiance biases for the High Resolution Infrared Radiation Sounders (HIRS) onboard NOAA-15, -16, and -17 from simultaneous nadir observations. *J. Atmos. and Ocn. Tech.*, **22**, 381-395.

Cao, C., M. Weinreb, and H. Xu, 2004: Predicting Simultaneous Nadir Overpasses among Polar-orbiting Meteorological Satellites for the Intersatellite Calibration of Radiometers. *J. Atmos. and Ocn. Tech.*, **21**, 537-542.

Cao, C. and A. K. Heidinger. 2002: Intercomparison of the longwave infrared channels of MODIS and AVHRR/NOAA-16 using simultaneous nadir observations at orbit intersections. In *Earth Observing Systems VII*, William L. Barnes (editor), Proceedings of SPIE, **4814**:306-316.

Cao C., M. Weinreb, and J. Sullivan, 2001, Solar Contamination Effects on the Infrared Channels of the AVHRR, *J. of Geophys. Res.,* **106**, D24, 33463-33469.

Guenther, B., W. Barnes, E. Knight, J. Barker, J. Harnden, R. Weber, M. Roberto, G. Godden, H. Montgomery, and P. Abel, 1996: MODIS Calibration: A brief review of the strategy for the at-launch calibration approach. *J. Atmos. and Ocn. Tech.*, **13**, 274-285.

Slater, P. N., S. F. Biggar, R. G. Holm, R. D. Jackson, Y. Mao, M. S. Moran, J. M. Palmer, and B. Yuan, 1987: Reflectance and radiance-based methods for the in-flight absolute calibration of multispectral sensors. *Remote Sens. Environ.*, **22**, 11-37.

Storch, H. V. and F. W. Zwiers, 2001: Statistical Analysis in Climate Research. Cambridge University Press, United Kingdom, 484 pp.